optica

Double grating shearing interferometry for X-ray free-electron laser beams: supplementary material

MIKAKO MAKITA[1,*], GEDIMINAS SENIUTINAS[2], MATTHEW H. SEABERG[3], HAE JA LEE[3], ERIC C. GALTIER[3], MENGNING LIANG[3], ANDREW AQUILA[3], SÉBASTIEN BOUTET[3], AKEL HASHIM[3], MARK S. HUNTER[3], TIM VAN DRIEL[3], ULF ZASTRAU[1], CHRISTIAN DAVID[2], AND BOB NAGLER[3,+]

[1]*European XFEL, Holzkoppel 4, 22869 Schenefeld, Germany*
[2]*Paul Scherrer Institut, Forschungsstrasse 111, 5232 Villigen PSI, Switzerland*
[3]*SLAC National Accelerator Laboratory, 2575 Sand Hill Road, Menlo Park, CA 94025, USA*
[*]*mikako.makita@xfel.eu*
[+]*bnagler@slac.stanford.edu*

Published 28 April 2020

This document provides supplementary information to "Double grating shearing interferometry for X-ray free-electron laser beams," https://doi.org/10.1364/OPTICA.390601. In a first section we give some additional information about the setup. The second section gives technical detail about the grating manufacturing. A third section gives the mathematical detail behind the interferograms and how they contain the phase information of the X-ray beam. In a final section, details of the shear inversion algorithm are given.

1. DETAILS OF THE SETUP

The diffraction gratings were mounted on 30 mm cage-mount systems, where one grating sits inside a motorised rotational holder, and another sits in a 2-axis lateral linear translation holder. Both gratings are manually positioned in distance and in the lateral positioning, using an optical microscope imaging system, prior to the x-ray measurement. The manual measurement of the grating distance was 0.7 mm to each other, and was further confirmed to be 0.68 mm by the analysis of the fringe orientation during the experiment. The whole unit was mounted on a motorised linear translation stage, which carries the gratings along the optical path of the focusing x-ray.

2. DETAILS OF THE DIFFRACTION GRATINGS

The diffraction gratings were fabricated at the Laboratory for Micro- and Nanotechnology at the Paul Scherrer Institut, Switzerland. The required grating pitch of 96 nm was calculated to allow for sufficient angular separation from the transmitted beam (angle β in Fig. 1 at 8.5 keV photon energy. The grating pattern was etched into a 10 μm thick diamond membrane provided by the Diamond Materials GmbH. Electron beam lithography was used to first print the grating patterns onto the mask layer on the membrane, over 614 µm $\times$ 614 µm area. The writing field of the electron beam exposure was set to 307 µm $\times$ 307 µm to reduce the number of stitching lines and still achieve the required resolution. The pattern was then transferred into the diamond by means of reactive ion etching (see Fig. S1 left), followed by Ir filling of the structure for 50-60 nm to increase the diffraction efficiency, using atomic layer deposition. This resulted in a checker-board grating made of Ir-filled diamond, with the structure depth of 300-400 nm, aspect ratio of approximately 10. The diffraction efficiency of the grating is found to be $\sim$1% of the main pulse energy (for the 1st orders), as estimated from the Pixis detector counts. Further details of such gratings can be found in [1, 2] .

During the experiment we took extra caution on the beam attenuation, as we were aware of the grating proximity to the sub-µm foci of KB mirrors. Generally the x-ray transmission level was kept at least at 10^{-5} or lower, for 120 Hz repetition rate. In this condition, no sign of contamination or damages to the structure were observed, either during or after the experiment with post-analysis using Scanning Electron Microscope (SEM). The only sign of damage was seen when we moved the grating through the focus to study the wavefront profile in the near-field region. Only at the focus, delamination of the grating structure 1.5 µm by 1.8 µm was confirmed, both from the disappearance of the signal and from the SEM image.

3. INTERFEROGRAMS

A two-dimensional checkerboard diffraction grating with circular pillars can be described as:

$$\mathrm{Ron}^{♔}(x,y) = T_1 + (T_2 - T_1)\,\square_\rho(x,y) + (T_2 - T_1)\,\square_\rho(x - \tfrac{D}{2}, y - \tfrac{D}{2}) \tag{S1}$$

with T_1 and T_2 the complex transmission function of the pillars and the rest of the substrate respectively and

$$\square_\rho(x,y) = \mathrm{circ}_\rho(x,y) \star Ш_D(x)\, Ш_D\,(y) \tag{S2}$$

the Dirac comb Ш is defined as

$$Ш_D\,(x) = \sum_{n=-\infty}^{+\infty} \delta(x - nD) \tag{S3}$$

The function $\mathrm{circ}_\rho(x,y)$ equals 1 inside the area of a circle with radius ρ, and 0 outside of it. We will need the Fourier transform of this function, which can be calculated easily in polar coordinates. Since the circ function has no dependence on the angle, the 2D fourier transform reduces to a Hankel transform of the radial coordinate, which can be evaluated in terms of a Bessel function:

$$\mathcal{F}[\mathrm{circ}_\rho(x,y)] = 2\pi \int_0^\infty \mathrm{circ}_\rho(x,y) J_0(\kappa r) r dr = \frac{2\pi r}{\kappa} J_1(\kappa r) \tag{S4}$$

with r the radial polar coordinate, $\kappa = \sqrt{k_x^2 + k_y^2}$, and with J_0 and J_1 Bessel functions of the first kind of order 0 and 1 respectively. We can now write the Fourier transform of the grating as :

$$\mathcal{R}^{♔}(k_x,k_y) = \sum_{l,m=-\infty}^{+\infty} R^{♔}_{l,m} \delta(k_x - k_l)\delta(k_y - k_m) \tag{S5}$$

with

$$k_l = \frac{2\pi}{D} l \quad \text{with } l \in \mathbb{Z} \tag{S6}$$

$$k_m = \frac{2\pi}{D} m \quad \text{with } m \in \mathbb{Z} \tag{S7}$$

$$\tag{S8}$$

with

$$R^{♔}_{l,m} = \begin{cases} (2\pi)^2 T_1 + (T_2 - T_1)(2\pi)^3 \tau^2 & \text{if } l = m = 0 \\ (T_2 - T_1)\frac{(2\pi)^2 \tau}{\eta_{lm}} J_1(2\pi \eta_{lm} \tau)[1 + e^{i\pi(l+m)}] & \text{otherwise} \end{cases} \tag{S9}$$

which is only non-zero when both l and m are odd, and with

$$\eta_{lm} = \sqrt{l^2 + m^2} \tag{S10}$$

$$\tau = \frac{\rho}{D} \tag{S11}$$

The checkerboard and its Fourier transform can be seen in Fig. S1.

These equations are valid if the checkerboard is aligned according to the XY axis. If we rotate it by angle alpha, the positions of the Dirac delta functions will not align with the axes of our coordinate system any more, and we need to write more generally:

$$\mathcal{R}^{♔}_\alpha(k_x,k_y) = \sum_{l,m=-\infty}^{+\infty} R^{♔}_{l,m} \delta(k_x - k^x_{lm})\delta(k_y - k^y_{lm}) \tag{S12}$$

with

$$\begin{bmatrix} k^x_{lm} \\ k^y_{lm} \end{bmatrix} = \begin{bmatrix} \cos\alpha & -\sin\alpha \\ \sin\alpha & \cos\alpha \end{bmatrix} \begin{bmatrix} k_l \\ k_m \end{bmatrix} \tag{S13}$$

The approach we now follow is similar to [3]. We first consider the electric field of a beam focused at $z = 0$, with electric field $E_0(x,y,0)$, and calculate using the paraxial approximation and the Fresnel integral its field at the camera position $z_2 = z_c$:

$$E_{c0}(x,y) = P_{z_c}(x,y) E^F_{c0}(x,y) \tag{S14}$$

with

$$E^F_{c0}(x,y) = -\frac{ik}{2\pi z_c} e^{ikz_c} \mathcal{F}\left[E_0(x,y) P_{z_c}(x,y)\right]_{\substack{k_x = \frac{k.x}{z_c} \\ k_y = \frac{k.y}{z_c}}} \tag{S15}$$

with k the wavenumber of the electromagnetic field and the spherical phase factor P_{z_c} defined as:

$$P_{z_c}(x,y) = \exp\left(\frac{ik}{2z_c}(x^2 + y^2)\right) \tag{S16}$$

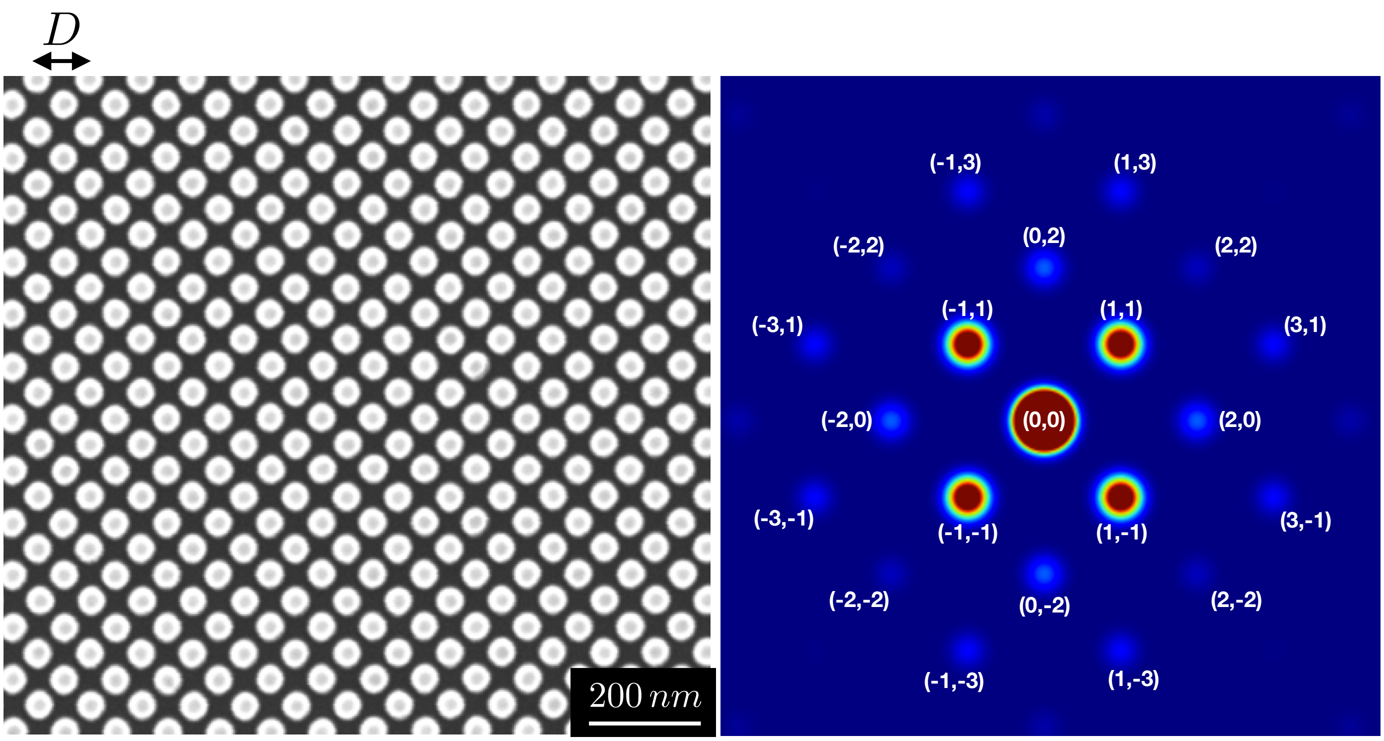

Fig. S1. SEM image of the checkerboard grating before Ir filling (left) and its Fourier transform (right) indexed in (l, m). The Fourier transform is convoluted with a Gaussian (equivalent to an incoming Gaussian beam on the checkboard grating) for visibility. The Ronchi shearing effect remains the same for square-profile checker board or a circular-profiles such as the one presented here. In this experiment the circular pillar structure is used, due to fabrication limits in maintaining sharp-edged profiles for small (< 200nm) pitch structures.

Essentially, E^F_{c0} is the electric field at the camera position with its spherical phase removed (i.e. with 'Flat' wavefront). We now place a checkerboard grating at position z_1 and propagate E_0 to that positions, multiply by the complex transmission function of the grating, and propagate the field back to the virtual focus using the Fresnel integral, and finally propagate this field to the camera plane at z_2. If we chose the orientation of the coordinate system such that the checkerboard is aligned with the axes we get (see also [3]):

$$E_{Rc} = (\frac{1}{2\pi})^2 P_{z_c}(x,y) \sum_{l,m=-\infty}^{+\infty} R^{♕}_{lm} e^{i(\phi_l+\phi_m)} E^F_{c0}(x - X^l_D, y - Y^m_D, z_c) \exp\left(i(k_l\, x + k_m\, y)\frac{z_1}{z_c} x\right) \tag{S17}$$

with

$$\phi_l = \frac{k_l^2 z_1}{2k}\left(\frac{z_1}{z_c} - 1\right) \tag{S18}$$

$$X^l_D = Y^l_D = \frac{k_l}{k}(z_c - z_1) \tag{S19}$$

In principle we could do this process again with the second grating, but the mathematics would become overly burdensome for our needs. Instead we will only consider the diffraction of the second grating of the transmitted beam (i.e. zero order) of the first grating (i.e. we will neglect for example the first order diffraction of the first grating being diffracted again in first order by the second grating). This is a reasonable assumption since the gratings only have a few percent efficiency in the first order, and less in the higher orders. Also, since we are interested only in the interference of the first order with each other, we will limit ourselves to these from now on. As the second grating is rotated with an angle α with respect to the first, we have to use Eq. (S12) and (S13). For the order $(l, m) = (1, 1)$ we get:

$$E^{11}_{R2} = (\frac{1}{2\pi})^2 P_{z_c}(x,y) R^{♕}_{11} e^{i\phi_{11}} E^F_{c0}(x - X^{11}_D, y - Y^{11}_D, z_c) \exp\left(i(k^x_{11}\, x + k^y_{11}\, y)\frac{z_1+\ell}{z_c} x\right) \tag{S20}$$

with

$$\phi_{11} = \left[(k^x_{11})^2 + (k^y_{11})^2\right] \frac{z_1+\ell}{2k}\left(\frac{z_1+\ell}{z_c} - 1\right) \tag{S21}$$

$$X^{11}_D = \frac{k^x_{11}}{k}(z_c - z_1 - \ell) \tag{S22}$$

$$Y^{11}_D = \frac{k^y_{11}}{k}(z_c - z_1 - \ell) \tag{S23}$$

We now take the phase difference between Eq. (S20) and the corresponding order of Eq. (S17). We ignore the constant phase term, as it has no practical importance. The linear term in x and y gives rise to the linear fringes, and for small angle α can easily be shown to correspond to Eq.1 with $\tan\beta = \frac{\sqrt{2}k_1}{k}$ the diffraction angle of the $(1,1)$ order, and with the shear direction $\bar{s}$ at -45 degrees. The last term in the phase difference equals

$$\phi^F_{c0}(x - X^1_D, y - Y^1_D, z_c) - \phi^F_{c0}(x - X^{11}_D, y - Y^{11}_D, z_c) \tag{S24}$$

Shifting the origin of x,y axis to the first order, this indeed reduces to

$$\hat{S}_{\bar{s}}\left(\phi_0(x, y)\right) = \phi_0(x, y) - \phi_0(x - s_x, y - s_y) \tag{S25}$$

with

$$\bar{s} = \left(X^{11}_D - X^1_D, Y^{11}_D - Y^1_D\right) \tag{S26}$$

which can easily be shown to be oriented at -45 degrees. The other first orders (i.e. $(l, m) = (1, -1)$, $(-1, 1)$ and $(-1, -1)$) can be treated analogously.

4. INVERTING THE SHEAR OPERATOR

To invert the shear operation, we use a method form [4] and elaborated in [3], which we adapt slightly to include non-integer values of the shear vector $\bar{s} = (s_x, s_y)$. We have a cost function :

$$U^2 = \sum_{\bar{s}} U^2_{\bar{s}} + \lambda\left(R^2_x + R^2_y\right) \tag{S27}$$

with

$$U^2_{\bar{s}} = \sum_{i,j}\left(\hat{S}_{\bar{s}}[\phi_{i,j}] - \phi^{\bar{s}}_{i,j} + \phi^{\bar{s}}_c\right)^2 P^{\bar{s}}_{i,j} \tag{S28}$$

The shear operator is defined as

$$\hat{S}_{\bar{s}}[\phi_{i,j}] = \phi_{i,j} - \hat{d}_{\bar{s}}[\phi_{i,j}] \tag{S29}$$

with the shift operator $\hat{d}_{\bar{s}}$ given by

$$\hat{d}_{\bar{s}}[\phi(x, y)] = \phi(x - s_x, y - s_y) \tag{S30}$$

R_x and R_y are added to the cost function to regularize for smoothness and defined as:

$$R^2_x = \sum_{i,j}\left(\phi_{i-1,j} - 2\phi_{i,j} + \phi_{i+1,j}\right)^2 P_{i-1,j}P_{i+1,j} \tag{S31}$$

$$R^2_y = \sum_{i,j}\left(\phi_{i,j-1} - 2\phi_{i,j} + \phi_{i,j+1}\right)^2 P_{i,,j-1}P_{i,,j+1} \tag{S32}$$

and λ is a regularization parameter. Since the shift parameter is unitary, we can show that the partial derivatives are equal to:

$$\frac{\partial U^2}{\partial\phi_{k,l}} = \sum_{\bar{s}}\frac{\partial U^2_{\bar{s}}}{\partial\phi_{k,l}} + \lambda\left(\frac{\partial R^2_x}{\partial\phi_{k,l}} + \frac{\partial R^2_y}{\partial\phi_{k,l}}\right) \tag{S33}$$

$$\frac{\partial U^2}{\partial\phi^{\bar{s}}_c} = 2\sum_{k,l} P^{\bar{s}}_{k,l}(\hat{S}_{\bar{s}}[\phi_{k,l}] - \phi^{\bar{s}}_{k,l} + \phi^{\bar{s}}_c) \tag{S34}$$

with

$$\frac{\partial U^2_{\bar{s}}}{\partial\phi_{k,l}} = 2\hat{S}_{-\bar{s}}\left[\left(\hat{S}_{\bar{s}}[\phi_{k,l}] - \phi^{\bar{s}}_{k,l} + \phi^{\bar{s}}_c\right)P^{\bar{s}}_{k,l}\right] \tag{S35}$$

$$\begin{aligned}\frac{\partial R^2_x}{\partial\phi_{k,l}} =& 2\left(\phi_{k,l} - 2\phi_{k+1,l} + \phi_{k+2,l}\right)P_{k,l}P_{k+2,l}\\ &- 4\left(\phi_{k-1,l} - 2\phi_{k,l} + \phi_{k+1,l}\right)P_{k-1,l}P_{k+1,l}\\ &+ 2\left(\phi_{k-2,l} - 2\phi_{k-1,l} + \phi_{k,l}\right)P_{k-2,l}P_{k,l}\end{aligned} \tag{S36}$$

$$\begin{aligned}\frac{\partial R^2_y}{\partial\phi_{k,l}} =& 2\left(\phi_{k,l} - 2\phi_{k,l+1} + \phi_{k,l+2}\right)P_{k,l}P_{k,l+2}\\ &- 4\left(\phi_{k,l-1} - 2\phi_{k,l} + \phi_{k,l+1}\right)P_{k,l-1}P_{k,l+1}\\ &+ 2\left(\phi_{k,l-2} - 2\phi_{k,l-1} + \phi_{k,l}\right)P_{k,l-2}P_{k,l}\end{aligned} \tag{S37}$$

These equation can be used for non-integer shear values, where we use an interpolated form of the shift function (e.g. bilinear, or bi-quadratic interpolation).

REFERENCES

1. C. David, S. Gorelick, S. Rutishauser, J. Krzywinski, J. Vila-Comamala, V. A. Guzenko, O. Bunk, E. Färm, M. Ritala, M. Cammarata, D. M. Fritz, R. Barrett, L. Samoylova, J. Grünert, and H. Sinn, "Nanofocusing of hard X-ray free electron laser pulses using diamond based Fresnel zone plates," Sci. Reports **1**, 57 (2011).
2. M. Makita, P. Karvinen, V. Guzenko, N. Kujala, P. Vagovic, and C. David, "Fabrication of diamond diffraction gratings for experiments with intense hard x-rays," Microelectron. Eng. **176**, 75 – 78 (2017).
3. B. Nagler, A. Aquila, S. Boutet, E. C. Galtier, A. Hashim, M. S. Hunter, M. Liang, A. E. Sakdinawat, C. G. Schroer, A. Schropp, M. H. Seaberg, F. Seiboth, T. van Driel, Z. Xing, Y. Liu, and H. J. Lee, "Focal spot and wavefront sensing of an x-ray free electron laser using ronchi shearing interferometry," Sci. Reports **7**, 13698 (2017).
4. M. Servin, D. Malacara, and J. L. Marroquin, "Wave-front recovery from two orthogonal sheared interferometers," Appl. Opt. **35**, 4343–4348 (1996).